Hyperfine structure of the $7d\ ^2D_{3/2}$ level in cesium measured by Doppler-free two-photon spectroscopy

P. V. Kiran Kumar, M. Sankari, and M. V. Suryanarayana*

National Centre for Compositional Characterisation of Materials, Bhabha Atomic Research Centre, Hyderabad-500 062, India

(Received 6 July 2012; published 9 January 2013)

We report the measurement of the hyperfine structure in the $7d\ ^2D_{3/2}$ state of ^{133}Cs isotope by Doppler-free two-photon fluorescence spectroscopy in a gas cell. The hyperfine level separations were measured using a frequency-stabilized Ti:sapphire laser locked to one of the hyperfine transitions and an acousto-optic modulator locked to another hyperfine transition. The frequency separation between various hyperfine levels has been measured with a precision of ∼100 kHz. From the measured hyperfine separations of the excited state, we have determined the magnetic dipole coupling constant (A) and electric quadrupole coupling constant (B) for the $7d\ ^2D_{3/2}$ state. The determined hyperfine structure constants are $A = 7.38\ (0.01)$ MHz and $B = -0.18\ (0.1)$ MHz. The values measured are found to be in good agreement with the earlier reported results using stepwise excitation process.

DOI: 10.1103/PhysRevA.87.012503 PACS number(s): 32.10.Fn, 32.30.−r, 42.62.Fi, 42.62.Eh

I. INTRODUCTION

In the recent past, there has been greater interest in the precision measurement and accurate determination of the excited-state properties of atomic systems [1–5]. The hyperfine splitting (HFS) results from electron-nuclear interactions and hence, the strength of the magnetic dipole, electric quadrupole, and magnetic octopole interactions between the nucleus and the orbital electrons can be determined from the measurements of the hyperfine splittings [6]. Further, measurement of the lifetime of excited states and their hyperfine splitting can help in the construction and modification of the atomic wave functions. They are particularly important while making a careful comparison of the experimental data with the theoretical predictions [7]. Comprehensive research [8] on the hyperfine structures of alkali elements has been carried out and their spectroscopic investigations have been a matter of considerable interest. Recently, there has been a renewed interest in the hyperfine structures of alkali atoms, and various groups have carried out experiments on the atomic structure of Cs. [4,9–14]. Precision measurements in Cs can lead to greater understanding of atomic and fundamental physics, including current measurement on atomic parity violation [15], search for the permanent electric dipole moment of an electron [16], and also help in the determination of the fine structure constant by photon recoil measurements [17]. Extensive precision measurements on the excited states of ^{133}Cs have been reported by Doppler-free two-photon spectroscopy [18–28]. Fendel *et al.* [23] have recently used the optical-frequency comb spectroscopy technique to determine the absolute frequency of the $6s\ ^2S_{1/2} \rightarrow 8s\ ^2S_{1/2}$ transition. Precision measurements of the hyperfine splitting of the $6d\ ^2D_{3/2,5/2}$ have been carried out using two-photon spectroscopy and also by the stepwise excitation process [4,29–31].

Belin *et al.* [32] have determined the magnetic dipole coupling constant of the Cs $7d\ ^2D_{3/2}$ state with a two-step level-crossing excitation process using a rf lamp and a cw dye laser. The accurate energies of nS, nP, nD, nF, and nG levels of neutral Cs have been determined by using non-resonant and resonantly enhanced Doppler-free two-photon spectroscopy [33]. The experimental and theoretical study on the polarizabilities and hyperfine structure constants of the $7d\ ^2D_{3/2,D_5/2}$ states in Cs has been carried out by Auzinsh *et al.* [34,35]. The measurement of the $7d\ ^2D_{3/2}$ hyperfine splitting intervals with resonant two-photon laser-induced fluorescence of an effusive beam of atomic Cs has been carried out by Kortyna *et al.* [36]. In this study, a radio-frequency phase modulation technique directly references the relative frequency scale to the ground hyperfine splitting of ^{87}Rb. The absolute transition frequencies and hyperfine coupling constants for the $8s\ ^2S_{1/2}$, $9s\ ^2S_{1/2}$, $7d\ ^2D_{3/2}$, and $7d\ ^2D_{5/2}$ states in ^{133}Cs vapor have been determined with high precision by stepwise excitation through either the $6p\ ^2P_{1/2}$ or $6p\ ^2P_{3/2}$ intermediate states with broadband laser light from a stabilized femtosecond laser optical-frequency comb [37]. The measurement of the hyperfine structure constants of the $7d\ ^2D_{3/2}$ and $7d\ ^2D_{5/2}$ states in Cs has been reported by Lee *et al.* by Doppler-free two-photon spectroscopy [27] using an electro-optic modulator for frequency calibration.

Recently, we have carried out the measurement of the transition isotope shift, hyperfine splittings, and the magnetic dipole constant (A) for the excited $6s\ ^2S_{1/2}$ state of both the isotopes of atomic potassium using an electro-optic modulator technique [38]. We have also measured the hyperfine splitting between the two hyperfine components and have also determined the magnetic dipole coupling constant (A) for the excited $9s\ ^2S_{1/2}$ state for the ^{133}Cs isotope [28].

The ground state of Cs is not directly coupled to the nd states via electric-dipole transition; therefore, we use the two-photon excitation process to access the $7d\ ^2D_{3/2}$ state. In this paper, the hyperfine splitting of Cs $7d\ ^2D_{3/2}$ was measured with an improved precision by using Doppler-free two-photon spectroscopy. We have adopted a locking technique to measure hyperfine splitting. A frequency-stabilized Ti:sapphire laser is locked to one of the hyperfine transitions and an acousto-optic modulator is locked to another hyperfine transition, thus enabling direct measurement of the frequency separation between the two hyperfine transitions. In general, by locking

*Corresponding author: surya@cccm.gov.in

the laser to an atomic reference, the center frequency can at best be measured to an accuracy of 1/100 of peak width [39]. Considering the peak width of about 2 MHz, the locking accuracy is expected to be about 20 kHz. The technique utilized in the current paper has been extensively applied for measurements of hyperfine structure of alkali elements in single-photon transitions by Natarajan and his co-workers [40–42], who have consistently achieved a precision better than 20 kHz. Though this technique requires utilization of identical setups, it provides good precision in measurements of the separations between various hyperfine components. Rapol *et al.* [40] have reported that, though the stability of the laser lock by a similar technique is only of the order of 1/20 of the line center, they could still achieve high precision because fluctuations of the two laser beams are correlated since they are derived from the same laser. The additional advantage of the current technique is that we can minimize the systematic errors by varying the locking frequency across various components of the hyperfine spectrum. We have determined both the hyperfine coupling constants (A and B) for the excited $7d\ ^2D_{3/2}$ state. We have also compared our results with earlier measurements carried out by stepwise excitation through an intermediate state using radio-frequency phase modulation technique [36], femtosecond-frequency comb technique [37], and also Doppler-free two-photon spectroscopy [27].

II. EXPERIMENT

The schematic of the experimental setup for the measurement of hyperfine splitting of the excited $7d\ ^2D_{3/2}$ state of cesium in a gas cell is shown in Fig. 1. Light, resonant with the $6s\ ^2S_{1/2} \rightarrow 7d\ ^2D_{3/2}$ transition by absorption of two photons at 767.8 nm was generated by a cw ring Ti:sapphire laser pumped by a 10-W diode-pumped solid-state (DPSS) laser.

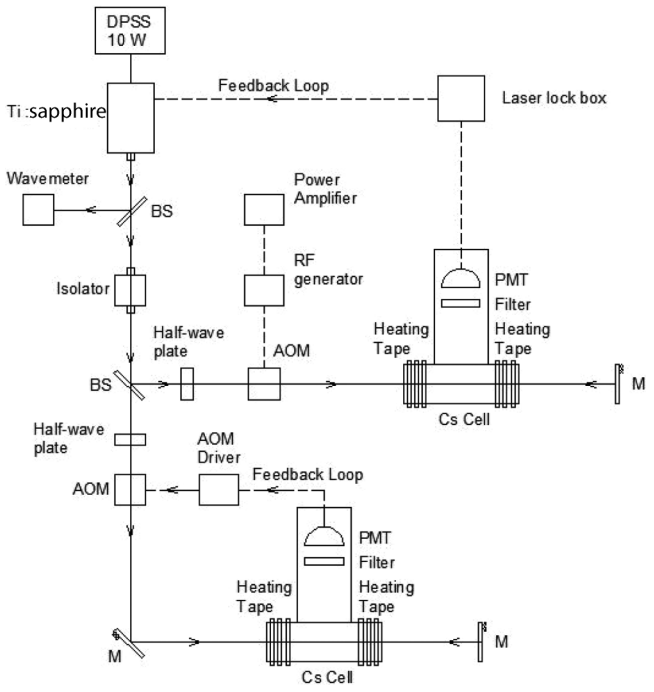

FIG. 1. Schematic of the experimental configuration.

The Ti:sapphire laser was actively stabilized to a thermally insulated reference cavity having a free spectral range of 750 MHz and a finesse >200 to reduce its frequency jitter to ∼60 kHz.

Two sealed Pyrex cells containing cesium were used for the experiments and the cells were maintained at about 100 °C, while the finger temperature was maintained at about 10 °C–15 °C lower than the cell to avoid coating of Cs vapor on the window. The Cs cell has been covered with a special two-layer magnetic shield (μ metal) to reduce the stray magnetic field to the level of ∼10 mG. The laser beam from the Ti:sapphire laser was retroreflected into the Cs gas cell. The overlap of the forward- and the retroreflected beams was optimized by maximizing the two-photon signal. A small fraction of the laser beam is fed to a wavemeter for monitoring the laser wavelength. In the Cs gas cell, the laser beam diameter is estimated to be about 2 mm and the laser power is about 150 mW, corresponding to a power density of ∼4.8 W/cm^2.

The atoms excited to the $7d\ ^2D_{3/2}$ state through the $6s\ ^2S_{1/2} \rightarrow 7d\ ^2D_{3/2}$ two-photon transition decay to the $7p\ ^2P_{1/2}$ and the $7p\ ^2P_{3/2}$ by emitting photons at ∼2334.6 and 2437.6 nm, respectively, and further cascade to the lower $6s\ ^2S_{1/2}$ state by emitting photons at ∼455.5 and 459.3 nm, respectively. The fluorescence signal was monitored using a photomultiplier tube (PMT) fitted with an interference filter centered at 450 nm and having a bandpass of 40 nm. The bias voltage applied to the PMT was typically about −800 V. Prior to carrying out any frequency measurements, the signal-to-noise (S/N) ratio was optimized to better than 100 for all the measurements. The output of the single-mode cw laser was split into two beams of equal power and is used for two different Doppler-free two-photon setups in two identical Cs gas cells. Two acousto-optic modulators (AOMs) are used for shifting the laser frequencies to precisely known values ($\nu_{\mathrm{aom}\,1}$ and $\nu_{\mathrm{aom}\,2}$) based on the separations between the hyperfine components. We have adopted three different approaches for measuring the hyperfine separations. They are (i) the frequency shifting technique, (ii) the wavemeter method, and (iii) the AOM locking technique. The detailed description of each of these methods has been described in their respective sections.

III. RESULTS AND DISCUSSION

The Cs atoms in a gas cell absorb two photons, i.e., one photon from the forward laser beam and another photon from the retroreflected beam, to excite Cs atoms from the ground $6s\ ^2S_{1/2}$ state to the $7d\ ^2D_{3/2}$ state. Since the nuclear spin (I) for the ^{133}Cs isotope is 7/2, for the S-D two-photon transition, two sets of four hyperfine transitions originating from the ground $F = 3$ level and $F = 4$ level to the upper levels $F' = 2,3,4$, and 5 are feasible according to the two-photon selection rules (Fig. 2). A typical Doppler-free two-photon spectrum recorded for the $6s\ ^2S_{1/2} \rightarrow 7d\ ^2D_{3/2}$ transition is depicted in Fig. 3.

A. Frequency shifting technique

The full width at half maximum (FWHM) of the hyperfine transitions has been measured by relatively shifting the frequencies of the two acousto-optic modulators by ∼5 MHz. The laser frequency into the first cell is upshifted by 110 MHz

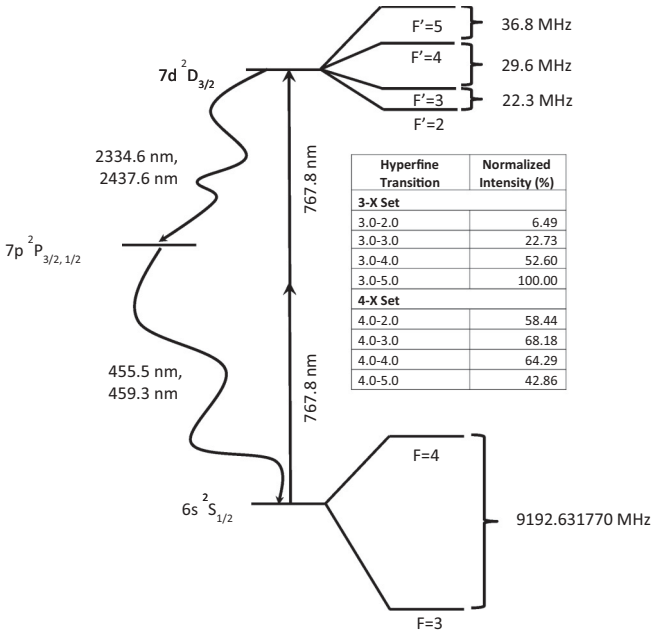

Hyperfine Transition	Normalized Intensity (%)
3-X Set	
3.0-2.0	6.49
3.0-3.0	22.73
3.0-4.0	52.60
3.0-5.0	100.00
4-X Set	
4.0-2.0	58.44
4.0-3.0	68.18
4.0-4.0	64.29
4.0-5.0	42.86

FIG. 2. Partial energy level diagram of Cs (not to scale).

($\nu_{\mathrm{aom}\,1}$) using an acousto-optic modulator while the frequency into the second Cs cell is upshifted by 105 MHz ($\nu_{\mathrm{aom}\,2}$) using another AOM, thus resulting in a precise relative shift of 5 MHz $\pm$ 1 Hz between the same hyperfine transitions in two cells (Fig. 4). With this accurately known relative frequency shift, we have estimated the linewidth of hyperfine transitions. The spectral width is measured to be $\sim$1.8 MHz by fitting the Lorentzian peaks to the experimental data. The contribution from the natural broadening due to the lifetime (160 ns) of Cs $7d\ ^2D_{3/2}$ state was estimated to be $\sim$1.0 MHz [43] and the rest could be ascribed either to the residual Doppler broadening due to imperfect overlap of the two counterpropagating laser beams or to the residual magnetic field causing Zeeman broadening. It is perhaps relevant to note that the spectral resolution of the hyperfine transitions was reported to be 3 MHz for the

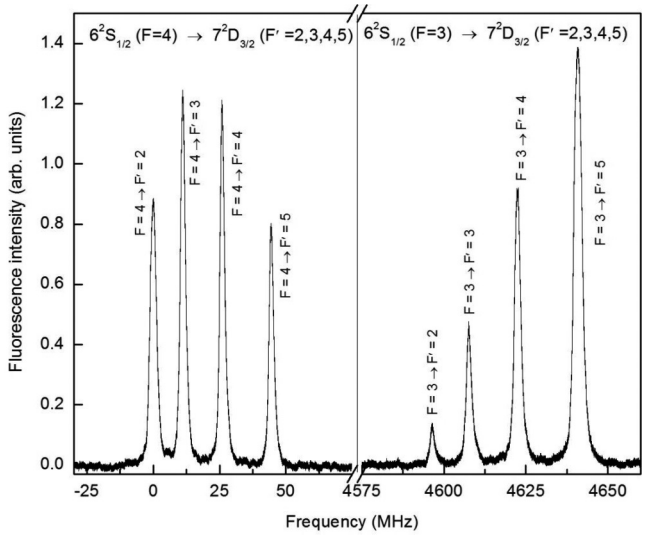

FIG. 3. The Doppler-free two-photon fluorescence spectrum for the $^2S_{1/2} \rightarrow 7d\ ^2D_{3/2}$ transition.

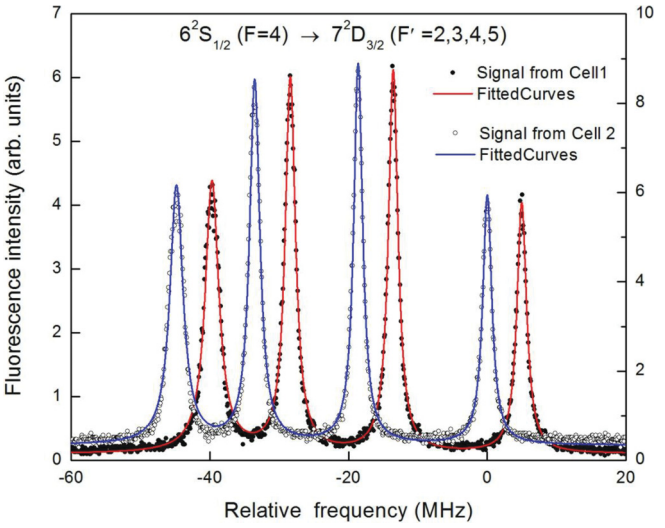

FIG. 4. (Color online) Two photon fluorescence spectrum of the $6s\ ^2S_{1/2}(F = 4) \rightarrow 7d\ ^2D_{3/2}(F' = 2,3,4,5)$ recorded with a 5MHz relative frequency shift.

$6s\ ^2S_{1/2} \rightarrow 7d\ ^2D_{3/2}$ two-photon transition carried out by Lee *et al.* [27]. It can be clearly observed that, in our study the S/N ratio is better and also the FWHM of the hyperfine transitions is significantly narrower than that reported earlier [27]. The hyperfine separations between the various levels have been determined using the relative shift of 5 MHz for frequency calibration. However, due to nonlinearity in the scan of the laser frequency, we could only achieve a precision of $\sim$500$-$600 kHz in our measurements.

B. Wavemeter method

Development of high-precision wavelength meters has made great progress in the recent past and presently commercial Fizeau-based wavelength meters are available which enable one to measure the absolute frequency to an accuracy of $\sim$2 MHz [44]. One significant advantage of these wavelength meters, compared with other available instruments, is the absence of any mechanical moving parts. However, relative frequencies can be measured with an accuracy of 500 kHz [28]. In the present study, a commercial wavemeter was utilized to initially measure the frequency of the hyperfine transition when the laser is locked to the fluorescence peak. To cross-check the hyperfine separations with the earlier reported results, the frequency of the laser is locked to the centers of various hyperfine components and the values are measured from a continuously calibrated commercial wavemeter. With our locking technique the laser frequency jitter is within 100 kHz. Normally, the center frequency of the line can be determined to a small fraction of the linewidth [39]. The measured hyperfine separations were found to be consistent with the earlier reported values of both Stalnaker *et al.* [37] and Kortyna *et al.* [36]. With this method we could measure the separations between various hyperfine transitions with a precision of 500 kHz. However, to improve the precision in the measurement of hyperfine separations, we have utilized the AOM locking technique adopted by Natarajan and his coworkers [40–42] to lock the constituent hyperfine components

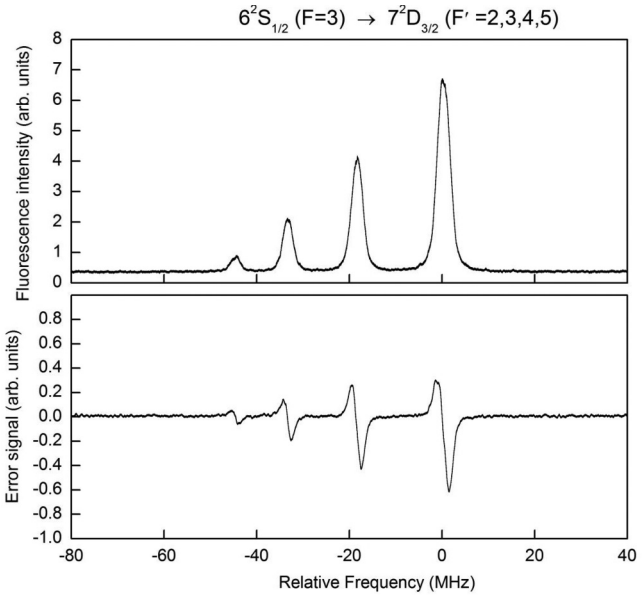

FIG. 5. The two photon fluorescence spectrum of the $6s\ ^2S_{1/2}(F=3) \rightarrow 7d\ ^2D_{3/2}(F'=2,3,4,5)$ along with the error signal.

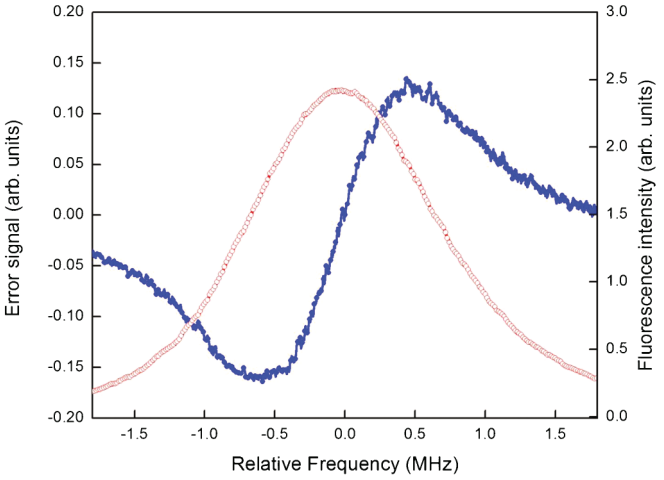

FIG. 6. (Color online) The fluorescence signal (circle) and the error signal (solid line) for the $6s\ ^2S_{1/2}(F=3) \rightarrow 7d\ ^2D_{3/2}(F'=4)$ recorded by scanning the AOM2. The laser is locked to the same hyperfine transition.

using an acousto-optic modulator (AOM); the details are discussed in the next section.

C. AOM locking technique

In this technique, the fluorescence signal in the first cell was used to lock the laser to one of the hyperfine transitions, while the fluorescence signal in the other cell is used for locking the AOM to another (or the same) hyperfine transition. The hyperfine separation is measured using the relation

$$\nu_{\mathrm{aom}\,2} - \nu_{\mathrm{aom}1} = \Delta\nu_{hfs}. \tag{1}$$

For these experiments, the error signal in the first cell has been generated by modulating the AOM frequency at $f_m =$ 25 kHz, using a commercial rf-signal generator whose internal clock is phase locked to a reference Rb oscillator having a short-term stability of $2 \times 10^{-11}\Delta\nu/\nu$ per second and long-term accuracy of $5 \times 10^{-10}\Delta\nu/\nu$ per year. The error signal is obtained by phase-sensitive detection at the same modulation frequency (f_m). The time constant of the low-pass filter of the lock-in amplifier was chosen as 1 ms with a filtering slope of 24 dB/octave. A typical error signal along with the two-photon Doppler-free fluorescence spectrum is shown in Fig. 5.

The fluorescence signal from the second cell is also modulated at $f_m \approx 25$ kHz by modulating the voltage-controlled oscillator (VCO) that drives the AOM, and the demodulated output is fed back to the VCO of the AOM driver through a loop filter. This feedback acts as a servo loop and locks the AOM frequency ($\nu_{\mathrm{aom}\,2}$) to the frequency separation between the two hyperfine components. The demodulated fluorescence signal generates the error signal for locking the AOM to the fluorescence peak in cell 2. The observed error signal obtained by scanning the AOM is shown in Fig. 6, while the laser is locked to one of the hyperfine components in cell 1. The AOM frequency is measured using a frequency counter, which is also phase locked (or referenced) to a stabilized Rb oscillator. The rubidium frequency standard in turn is referenced to the ^{87}Rb $5s\ ^2S_{1/2}(F=1) \rightarrow 5s\ ^2S_{1/2}(F=2)$ ground hyperfine transition at 6 834 682 612.8 Hz. The hyperfine separations have been determined using Eq. (1).

As mentioned earlier, two sets of hyperfine transitions, i.e., $F = 3 \rightarrow (F' = 2,3,4,$ and 5) and $F = 4 \rightarrow (F' = 2,3,4,$ and 5), are possible according to two-photon selection rules. Due to the large hyperfine splitting of the $6s\ ^2S_{1/2}$ ground state of Cs (9192.631 770 MHz), the hyperfine transitions originating from ground $F = 3$ and $F = 4$ levels are well separated. Since, the same upper levels are populated in both sets of hyperfine transitions, the hyperfine structure constants can be measured with either set. Experiments have been carried out to measure hyperfine separations of $7d\ ^2D_{3/2}$ level using the hyperfine transitions originating from both $F = 3$ and $F = 4$ levels of $6s\ ^2S_{1/2}$. The hyperfine separations have been determined for all the six possible combinations, by locking the laser to each of the hyperfine transition in cell 1 and then locking the second AOM to the remaining three hyperfine transitions in cell 2. Since hyperfine separations have been measured for all the possible combinations, the results are expected to yield better accuracy. Each hyperfine interval is determined by averaging the measured AOM frequencies over 200–250 independent measurements, and the results have been repeatedly checked for their consistency over several days. This resulted in an overall statistical error of about 100 kHz in each value, except in the case of the hyperfine transition $F = 3 \rightarrow F' = 2$ where the precision was about 150 kHz. The larger uncertainty in the measured separation between these two components is primarily due to the smaller intensity of the $F = 3 \rightarrow F' = 2$ hyperfine component. Further, we have interchanged the laser locking (cell 1 to cell 2) and AOM locking (cell 2 to cell 1) and have repeated the entire set of measurements for this configuration. The measured frequency separations between the various hyperfine levels from both these configurations are found to be consistent with each other within a statistical uncertainty of $<$100 kHz. The average values of the hyperfine

TABLE I. The measured hyperfine separations between the various hyperfine levels of the $7d\ ^2D_{3/2}$ level of cesium for the present work along with the earlier reported results.

Hyperfine interval of the $7d\ ^2D_{3/2}$ level of cesium	Measured (this work) (MHz)	Reference [27] (MHz)	Reference [37][a] (MHz)	Reference [36] (MHz)
$F' = 5 \rightarrow F' = 4$	36.93 (0.08)	37.28 (0.25)	36.80	37.0 (0.20)
$F' = 5 \rightarrow F' = 3$	66.30 (0.08)	67.49 (0.43)[b]	66.40	66.2 (0.28)[b]
$F' = 5 \rightarrow F' = 2$	88.59 (0.11)	90.50 (0.32)[b]	88.68	88.4 (0.28)[b]
$F' = 4 \rightarrow F' = 3$	29.59 (0.08)	30.21 (0.35)	29.60	29.2 (0.20)
$F' = 4 \rightarrow F' = 2$	51.79 (0.09)	53.22 (0.40)[b]	51.88	51.4 (0.28)[b]
$F' = 3 \rightarrow F' = 2$	22.49 (0.15)	23.01 (0.20)	22.29	22.2 (0.20)

[a]The separations have been calculated from the reported A and B values.
[b]These separations have been deduced from the experimentally measured separations of consecutive hyperfine transitions.

separations along with the previously measured values from the literature are listed in Table I.

We have also verified the lock point tracking of the *master-slave* system, by gradually varying the frequency of first AOM from 110 to 120 MHz, and thus checked the tracking of the slave lock in cell 2. Within the range of 10 MHz, the second AOM has been found to consistently follow the AOM frequency in the first cell, resulting in a precision of 50–100 kHz for all the measurements.

It can be observed from Table I that the measured hyperfine separations are in good agreement with the results of Stalnaker *et al.* [37] and Kortyna *et al.* [36], except for the $F = 3 \rightarrow F' = 2$ transition, whereas our results deviate from the reported values of Lee *et al.* [27] by more than 350–600 kHz. From the initial observation of Table I, we find that our measured frequency separations deviate from the separations of Kortyna *et al.* [36] by ~70–400 kHz; however, by considering an effective standard deviation (σ) for each splitting and by combining the individual σ in quadrature, our measured hyperfine separations deviate from that of Kortyna *et al.* [36] by an average of only 0.9σ. It can also be observed that the measurements in the current study deviate from that of Stalnaker *et al.* [37] by 1.0σ, however, they deviate by an average of 2.8σ with that of Lee *et al.* Because of this insignificant difference (1.0σ), we conclude that our results are consistent with the earlier reported works of both Stalnaker *et al.* [37] and Kortyna *et al.* [36]. Our results also agree with Lee *et al.* [27] but at a much lower certainty.

Hyperfine separations measured by Kortyna *et al.* [36] deviate from Lee *et al.* [27], though both of them adopted a phase modulation technique wherein the electro-optic modulator (EOM) is used to generate sidebands for frequency calibration of laser frequency. The only difference is that Kortyna *et al.* [36] have used a stepwise excitation while Lee *et al.* [27] have used Doppler-free two-photon spectroscopy. Due to phase modulation, the atomic spectral features are reproduced at precise intervals. From our experience, such a method should be followed by an accurate and careful approach of identifying the calibration factor and a reliable peak fitting procedure to account for the nonlinearities in the laser scan to avoid erroneous results. Kortyna *et al.* [36] have utilized a calibration factor for individual sideband and the corresponding center frequency peak from six calibration factors per spectrum; they have carefully evaluated the linearity of the frequency scan and have made first-order correction in their data analysis procedure. For identifying the centroid of each peak they have used nonlinear fitting to locate the center. A Voigt profile has been fitted to each of the six peaks using a Levenberg-Marquardt residual minimization algorithm and a linear function to the background. Due to this accurate and reliable approach, their results were in good agreement by Stalnaker *et al.* [37], who have used a frequency comb technique for the measurements. Lee *et al.* [27] have probably overlooked this important aspect of accurately determining the proper calibration factor and rigorous peak fitting routine while analyzing their data.

It is evident that though Lee *et al.* [27] have carried out nonlinear fitting to identify the center of each fluorescence peak, the uncertainty arising solely from the frequency-scale calibration was 200 kHz leading to a total uncertainty of 250 kHz. It is noteworthy to observe that Kortyna *et al.* [36] have reported the overall uncertainty as 200 kHz, which is comprised of the quadrature sum of the statistical uncertainty, the centroid uncertainty due to the fitting algorithm, and the calibration uncertainty due to jitter in the calibration procedure. Moreover, the hyperfine separations reported by Lee *et al.* [27] are consistently higher than the present work, and also higher than the values quoted by Kortyna *et al.* [36] and Stalnaker *et al.* [37] by 350–600 kHz, indicating a probable unknown source of error in either their measurements or data analysis. The experimental approach discussed in this paper differs significantly from that adopted by both Lee *et al.* [27] and Kortyna *et al.* [36]. On the contrary, in our case, due to the smaller peak widths (~1.8 MHz), it is possible to lock to the peak of each hyperfine component within an uncertainty of <100 kHz using the locking technique. Since the hyperfine separations are measured from the difference frequencies of AOMs, the uncertainty is expected to be lower.

D. Analysis of the hyperfine spectrum of Cs

In a two-photon transition between a $^2S_{1/2}$ and a ^2D_j state, the two-photon transition operator is purely quadrupolar in nature [45] and the relative hyperfine line intensities between the two hyperfine components of the two different states is given by Ref. [46]

$$I(F_g \rightarrow F_e) \propto \frac{(2F_g + 1)(2F_e + 1)}{(2I + 1)} \begin{Bmatrix} J_e & 2 & J_g \\ F_g & I & F_e \end{Bmatrix}^2, \quad (2)$$

where J, I, and F are the electronic, nuclear, and total angular momentum quantum numbers, respectively [47,48]; the subscripts "g" and "e" denote the ground and the upper states. The energy of the hyperfine structure component (W_F) is given by the Casimir relation [48]

$$W_F = \frac{C}{2}A + \frac{3C(C+1) - 4I(I+1)J(J+1)}{8I(2I-1)J(2J-1)}B, \quad (3)$$

where $C = F(F+1) - I(I+1) - J(J+1)$.

The energy W_F of the hyperfine structure component is a function of two electromagnetic multipole terms, namely, the magnetic dipole moment (A) and the electric quadrupole moment (B).

After measuring the hyperfine separation between the various components of the $7d\ ^2D_{3/2}$ state of ^{133}Cs isotope, we have determined the magnetic dipole constant (A) and electric quadrupole coupling constant (B) for the $7d\ ^2D_{3/2}$ level. The hyperfine structure constants are determined by inserting the measured hyperfine intervals into the Casimir formula. A set of coupled linear equations for the hyperfine separations $\Delta W = W_{F''} - W_{F'}$ in terms of A and B for a nuclear spin of $I = 7/2$ and $J = 3/2$ are obtained and are listed below:

$$W_5 - W_4 = 5A + \tfrac{5}{7}B = 36.93\ (0.08), \quad (4)$$

$$W_5 - W_3 = 9A + \tfrac{3}{7}B = 66.30\ (0.08), \quad (5)$$

$$W_5 - W_2 = 12A - \tfrac{2}{7}B = 88.59\ (0.11), \quad (6)$$

$$W_4 - W_3 = 4A - \tfrac{2}{7}B = 29.59\ (0.08), \quad (7)$$

$$W_4 - W_2 = 7A - B = 51.79\ (0.09), \quad (8)$$

$$W_3 - W_2 = 3A - \tfrac{5}{7}B = 22.49\ (0.15), \quad (9)$$

where the quantities on the right-hand side of the coupled equations are the measured hyperfine separations.

Using the method of least-squares minimization, we determine the magnetic dipole coupling constant A and the electric quadrupole coupling constant B and we propagate the uncertainties through these formulas. In the present technique, unlike in earlier reports, we have measured all the six possible hyperfine separations between various hyperfine components. Hence, in the least-squares minimization routine, the values for A and B have been derived by inclusion of all the six hyperfine separations instead of three.

Before applying the minimization routine to our measured hyperfine separations, the least-squares minimization procedure has been evaluated for its correctness, by deducing the A, B constants from the measured hyperfine separations reported earlier [30,37]. The calculated hyperfine separations for the $7d\ ^2D_{3/2}$ state from the reported A and B values of Ref. [37] were used as the input parameters for the least-squares minimization routine. We could exactly deduce the A and B values reported by Stalnaker *et al.* [37]. In the case of Ref. [30], the calculated A and B values by our minimization routine were within an error of 10 kHz for the A value and ∼40 kHz for the B value.

TABLE II. The hyperfine coupling constants for the $7d\ ^2D_{3/2}$ state of cesium deduced from the hyperfine separations along with the earlier reported values.

Hyperfine coupling constants		
A (MHz)	B (MHz)	Reference
7.38 (0.01)	−0.18 (0.1)	This work
7.36 (0.07)	−0.88 (0.87)	Reference [27]
7.386 (0.015)	−0.18 (0.16)	Reference [37]
7.36 (0.03)	−0.1 (0.2)	Reference [36]

The least-squares minimization method has yielded the A value to be 16.33 MHz and the B value to be 0.14 MHz, while the reported values were 16.34 and 0.1 MHz, respectively. This difference is inconsequential when rounded off to the significant digits as mentioned in Ref. [30]. As mentioned earlier, it is noteworthy to observe that though the hyperfine separations (Table I) measured by Lee *et al.* [27] are relatively higher compared to the results of Kortyna *et al.* [36], Stalnaker *et al.* [37], and those of the present work, the deduced A and B values of Lee *et al.* from their measured hyperfine separations are unexpectedly in close agreement with the hyperfine coupling constants reported by Refs. [36] and [37]. We have utilized our least-squares minimization program for deducing the A and B values from the measured hyperfine separations of Lee *et al.* [27]. However, the obtained A and B values were significantly different from those reported by Lee *et al.* [27]. From our least-squares minimization routine the values were 7.53 and −0.54 MHz for A and B, respectively, while the reported values of Lee *et al.* were 7.36 and −0.88 MHz.

Agreement between the deduced A and B values from our minimization routine with those reported by Refs. [30] and [37] has given us enough confidence to proceed for the determination of hyperfine structure constants of the $7d\ ^2D_{3/2}$ level. After verification of the correctness of the minimization program, we have utilized this least-squares minimization program for deducing the A and B values from our measured hyperfine separations. Inclusion of six separations in the minimization routine predictably yields much more precise and accurate values for A and B. We have deduced the magnetic dipole coupling constant A and electric quadrupole constant B from the least-squares minimization of the coupled linear equations by inserting the measured hyperfine separations. The six measured hyperfine frequency separations in Table I have been utilized to deduce the magnetic dipole coupling constant A and electric quadrupole coupling constant B; the results are listed in Table II.

Our results are in good agreement with those of Stalnaker *et al.* [37] and Kortyna *et al.* [36], who have adopted a stepwise excitation through either the $6p\ ^2P_{1/2}$ or the $6p\ ^2P_{3/2}$ intermediate state. The measurement by Stalnaker *et al.* [37] is performed directly with a broadband laser light from a frequency-stabilized femtosecond laser optical-frequency comb, while the measurement by Kortyna *et al.* [36] is based on the radio-frequency phase modulation technique.

IV. SYSTEMATIC AND STATISTICAL ERRORS

A. Statistical errors

We briefly discuss the different sources of error in our measurements. The primary sources of statistical error are due to the fluctuations in the lock point of the laser and the AOM. To minimize these errors, we have used an integration time of 10 s for each measurement of the AOM frequency in the frequency counter. Additionally we have obtained the average value for about 200–250 measurements for a given transition, and have repeated the set several times on different days. This results in an overall statistical error of ∼100 kHz in each value.

B. Systematic errors

The possible systematic errors could be (i) the second-order Doppler effect, (ii) Zeeman shifts, (iii) the Stark shift (light shift caused by the electric field of the light in two-photon transitions), (iv) pressure shifts, and (v) peak pulling errors.

Two-photon spectroscopy eliminates the first-order Doppler effect but not the second-order term which is given by

$$\delta\upsilon = \left(\frac{u}{c}\right)^2 \upsilon. \tag{10}$$

For the case of Cs, for the $6s\ ^2S_{1/2} \rightarrow 7d\ ^2D_{3/2}$ transition, $\frac{u}{c}$ is 7.2×10^{-7} and $\nu = 780.89$ THz, and the magnitude of second-order Doppler shift is ∼410 Hz which is negligible compared to the other uncertainties in our measurements.

The effects of optical pumping and Zeeman shifts associated with the stray (or Earth's) magnetic field are one potential source of systematic error. The stray (or Earth's) magnetic field splits the Zeeman sublevels. Peak shifts occur due to optical pumping into Zeeman sublevels. This systematic shift of the peak of the hyperfine transition $|F,m_F\rangle \rightarrow |F',m_{F'}\rangle$ due to optical pumping can be calculated from the expression

$$\mu_B(g_{F'}m_{F'} - g_F m_F)B, \tag{11}$$

where the Bohr magneton $\mu_B = 1399.6$ kHz/G while g_F represents the Lande g factor for the two hyperfine levels of the transition, and B is the magnetic field. In the present experiments, we have utilized pure, linearly polarized light by utilizing PBS cubes with a high extinction ratio (T_p/T_s) of 1000:1. Since the two-photon excitation is carried out by a perfectly linearly polarized light, there will be no asymmetric pumping of the hyperfine transition and hence the line center will remain unaffected. We have also minimized the stray magnetic fields by surrounding the Cs cell with two layers of μ-metal shield to a level of 10 mG. Under such conditions, the Zeeman shift is expected to be less than 40 kHz.

The light shift (ac Stark shift) which is a disadvantage for a two-photon transition is proportional to the laser intensity and can be calculated from the expression

$$\text{Stark shift} = -\sum_i \left(\frac{\Omega_{2i}^2}{4\Delta_{2i}} - \frac{\Omega_{1i}^2}{4\Delta_{1i}}\right), \tag{12}$$

where Ω_{1i} and Ω_{2i} are the one-photon Rabi frequencies for the coupling of the intermediate state $|i\rangle$ with the ground state $|1\rangle$ and the final state $|2\rangle$, respectively. Δ_{ji} is the frequency detuning between the virtual and real intermediate levels and the summation is taken over all the real intermediate levels. This value can be evaluated by considering only the nearby intermediate levels which are close to the virtual level. The Rabi frequencies were evaluated using Einstein's spontaneous emission coefficients from the Kurucz database [49]. To calculate the ac Stark shift, we have considered the $6p\ ^2P_{1/2}$, $6p\ ^2P_{3/2}$, $7p\ ^2P_{1/2}$, $7p\ ^2P_{3/2}$ intermediate levels. The ac Stark shift was calculated to be ∼0.7 kHz for a laser intensity of 4.8 W/cm^2.

TABLE III. Magnitude of the contributions of systematic errors to the error budget.

Source of error	Magnitude (kHz)
Second-order Doppler shift	0.4
Zeeman shift	40
ac Stark shift	0.7
Pressure shift	12
Peak pulling shift	4

The other source of error could be the pressure (collisional) shift in the vapor cell. From the detailed study of shifts due to collisions by Stalnaker *et al.* [37], we expect the collisional shift to be about ∼12 kHz.

Peak pulling arises basically due to the shift in the peak due to wing overlap from the neighboring transitions. Peak pulling effects do contribute significantly, in particular for the situations where significant overlap exists between the neighboring atomic resonances and also for the cases where the atomic spectral features ride over the underlying Doppler profile. Peak pulling effects can also cause significant systematic errors if there is a substantial difference in the intensities of the peaks. For the case of $F = 4 \rightarrow (F' = 2,3,4,$ and 5) hyperfine transitions, the intensities of hyperfine transitions are nearly comparable, therefore, peak pulling effects are expected to be insignificant. However, for the $F = 3 \rightarrow (F' = 2,3,4,$ and 5) hyperfine transition set, there could be peak pulling effect for the $F = 3 \rightarrow F' = 2$ hyperfine transition causing systematic shift owing to the low intensity (6.49%) of the hyperfine transition. The peaks are also susceptible to being pulled away from the resonance when the line shape of the atomic resonance is significantly dependent on the Doppler broadening, which has a direct dependence on the temperature.

However, in the present case, the peaks due to Doppler-free two-photon excitation have a linewidth of ∼1.8 MHz which is much less than the smallest hyperfine separation of ∼11.4 MHz. Since these Doppler-free peaks are observed on a flat background, pulling effects for Doppler-free peaks are expected to be negligible. We have simulated the Doppler-free peaks and have estimated the peak pulling effects and these are found to be of the order of ∼4 kHz.

The various systematic errors considered for the calculation of the overall uncertainty have been shown in Table III. The average frequency separations between the various hyperfine transitions are measured with a total error of 108 kHz obtained by adding in quadrature all the systematic errors listed in Table III with a statistical error of 100 kHz. Since, the contribution from the systematic shifts to the overall error budget is ∼7%; we have ignored the contribution from systematic shifts in our measurements.

V. CONCLUSIONS

We have measured the hyperfine separations of the $7d\ ^2D_{3/2}$ using a Doppler-free two-photon transition for the $6s\ ^2S_{1/2} \rightarrow 7d\ ^2D_{3/2}$ in a Cs gas cell. The hyperfine separations have been measured by locking the laser to one of the hyperfine transitions using a Doppler-free two-photon technique, and an AOM was utilized to scan the stabilized laser about the resonance of the neighboring hyperfine transition (or another hyperfine transition) in another Doppler-free two-photon setup. The AOM is locked to this neighboring component and thus the difference in the two AOMs was utilized to measure the hyperfine separation between the two locked peaks. From the measurement of the hyperfine separations, we have derived the precise values of the magnetic dipole coupling constant and the electric quadrupole coupling constant of the $7d\ ^2D_{3/2}$ state. By utilizing this technique we could achieve a precision of $\sim$100 kHz for the frequency separations between the hyperfine levels. The A and B coupling constants agree with previous measurements, and to our knowledge the precision achieved by the current technique is so far the best in Doppler-free two-photon spectroscopy for the $7d\ ^2D_{3/2}$ state.

[1] U. Volz and H. Schmoranzer, Phys. Scr., T **63**, 48 (1996).
[2] J. E. Simsarian, W. Shi, L. A. Orozco, G. D. Sprouse, and W. Z. Zhao, Opt. Lett. **21**, 1939 (1996).
[3] B. Hoeling, J. R. Yeh, T. Takekoshi, and R. J. Knize, Opt. Lett. **21**, 74 (1996).
[4] N. Ph. Georgiades, E. S. Polzik, and H. J. Kimble, Opt. Lett. **19**, 1474 (1994).
[5] D. Sundholm and J. Olsen, Phys. Rev. Lett. **68**, 927 (1992).
[6] J. Lloyd, *Theory of the Hyperfine Structure of Free Atoms* (Wiley-Interscience, New York, 1971).
[7] C. L. Cesar, D. G. Fried, T. C. Killian, A. D. Polcyn, J. C. Sandberg, I. A. Yu, T. J. Greytak, D. Kleppner, and J. M. Doyle, Phys. Rev. Lett. **77**, 255 (1996).
[8] E. Arimondo, M. Inguscio, and P. Violino, Rev. Mod. Phys. **49**, 31 (1977).
[9] W. Yei, A. Sieradzan, E. Cerasuolo, and M. D. Havey, Phys. Rev. A **57**, 3419 (1998).
[10] Th. Udem, J. Reichert, T. W. Hansch, and M. Kourogi, Phys. Rev. A **62**, 031801 (2000).
[11] J. Guena, M. Lintz, and M. A. Bouchiat, Phys. Rev. A **71**, 042108 (2005).
[12] C. Fort, F. S. Cataliotti, P. Raspollini, G. M. Tino, and M. Inguscio, Z. Phys. D **34**, 91 (1995).
[13] R. J. Rafac and C. E. Tanner, Phys. Rev. A **56**, 1027 (1997).
[14] V. Gerginov, A. Derevianko, and C. E. Tanner, Phys. Rev. Lett. **91**, 072501 (2003).
[15] C. S. Wood, S. C. Bennett, D. Cho, B. P. Masterson, J. L. Roberts, C. E. Tanner, and C. E. Wieman, Science **275**, 1759 (1997).
[16] S. A. Murthy, D. Krause, Z. L. Li, and L. R. Hunter, Phys. Rev. Lett. **63**, 965 (1989).
[17] A. Wicht, J. M. Hensley, E. Sarajlic, and S. Chu, Phys. Scr., T **102**, 82 (2002).
[18] E. Campani, G. Degan, G. Gorini, and E. Polacco, Opt. Commun. **24**, 203 (1978).
[19] P. P. Herrmann, J. Hoffnagle, A. Pedroni, N. Schlumpf, and A. Weis, Opt. Commun. **56**, 22 (1985).
[20] M. Bellini, A. Bartoli, and T. W. Hansch, Opt. Lett. **22**, 540 (1997).
[21] G. Hagel, C. Nesi, L. Jozefowski, C. Schwob, F. Nez, and F. Biraben, Opt. Commun. **160**, 1 (1999).
[22] K. Sasaki, K. Sugiyama, V. Barychev, and A. Onae, Jpn. J. Appl. Phys. **39**, 5310 (2000).
[23] P. Fendel, S. D. Bergeson, Th. Udem, and T. W. Hänsch, Opt. Lett. **32**, 701 (2007).
[24] C. Y. Cheng, C. M. Wu, G. B. Liao, and W. Y. Cheng, Opt. Lett. **32**, 563 (2007).
[25] Y. C. Lee, Y. H. Chang, Y. Y. Chen, C. C. Tsai, and H. C. Chui, J. Phys. B **43**, 235003 (2010).
[26] Y. C. Lee, H. C. Chui, Y. Y. Chen, Y. H. Chang, and C. C. Tsai, Opt. Commun. **283**, 1788 (2010).
[27] Y. C. Lee, Y. H. Chang, Y. Y. Chen, H. C. Chui, and C. C. Tsai, Appl. Phys. B **105**, 391 (2011).
[28] P. V. Kiran Kumar and M. V. Suryanarayana, Opt. Commun. **285**, 1838 (2012).
[29] C. Tai, W. Happer, and R. Gupta, Phys. Rev. A **12**, 736 (1975).
[30] A. Kortyna, N. A. Masluk, and T. Bragdon, Phys. Rev. A **74**, 022503 (2006).
[31] A. Kortyna, C. Tinsman, J. Grab, M. S. Safronova, and U. I. Safronova, Phys. Rev. A **83**, 042511 (2011).
[32] G. Belin, L. Holmgren, and S. Svanberg, Phys. Scr. **14**, 39 (1976).
[33] K. H. Weber and C. J. Sansonetti, Phys. Rev. A **35**, 4650 (1987).
[34] M. Auzinsh, K. Blushs, R. Ferber, F. Gahbauer, A. Jarmola, and M. Tamanis, Opt. Commun. **264**, 333 (2006).
[35] M. Auzinsh, K. Bluss, R. Ferber, F. Gahbauer, A. Jarmola, M. S. Safronova, U. I. Safronova, and M. Tamanis, Phys. Rev. A **75**, 022502 (2007).
[36] A. Kortyna, V. Fiore, and J. Farrar, Phys. Rev. A **77**, 062505 (2008).
[37] J. E. Stalnaker, V. Mbele, V. Gerginov, T. M. Fortier, S. A. Diddams, L. Hollberg, and C. E. Tanner, Phys. Rev. A **81**, 043840 (2010).
[38] P. V. Kiran Kumar and M. V. Suryanarayana, J. Phys. B **44**, 055003 (2011).
[39] C. J. Foot, *Atomic Physics* (Oxford University Press, Oxford, 2005).
[40] U. D. Rapol, A. Krishna, and V. Natarajan, Eur. Phys. J. D **23**, 185 (2003).
[41] D. Das and V. Natarajan, J. Phys. B: At. Mol. Opt. Phys. **39**, 2013 (2006).
[42] D. Das and V. Natarajan, J. Phys. B: At. Mol. Opt. Phys. **40**, 035001 (2008).
[43] J. Marek, Phys. Lett. A **60**, 190 (1977).
[44] http://www.highfinesse.com/.

[45] B. Cagnac, G. Grynberg, and F. Biraben, J. Phys. **34**, 845 (1973).
[46] G. Grynberg, F. Biraben, E. Giacobino, and B. Cagnac, J. Phys. **38**, 629 (1977).
[47] I. I. Sobleman, *Atomic Spectra and Radiative Transitions* (Springer-Verlag, Berlin, 1979).
[48] G. K. Woodgate, *Elementary Atomic Structure*, 2nd ed. (Oxford University Press, Oxford, 1980).
[49] R. L. Kurucz and B. Bell, *Atomic Line Data Kurucz CD-ROM No. 23* (Smithsonian Astrophysical Observatory, Cambridge, MA, 1995).